SCATTERING OF OBLIQUE SURFACE WAVES BY PERMEABLE BARRIERS

By T. Sahoo,[1] A. T. Chan,[2] and A. T. Chwang,[3] Fellow, ASCE

ABSTRACT: The scattering of oblique incident surface waves by permeable vertical barriers in water of finite depth is investigated for four different barrier configurations: (1) A bottom-standing barrier; (2) a surface-piercing barrier; (3) a barrier with a gap; and (4) a submerged barrier. The boundary-value problems are converted to dual/triple series relations by suitable application of the eigenfunction expansion method, and then the full solutions are obtained by the least-square approximation method. The variations of reflection coefficients, hydrodynamic pressure differences along the two sides of the barriers, and surface elevations are obtained for different values of the wave-effect parameter, the porous-effect parameter, as well as the angle of incidence. It is observed that the finite angle of incidence as well as the porous effect of the barriers reduce the reflection of the incident waves imparted on the barriers, the wave amplitude, and the hydrodynamic pressure exerted on the barriers. 3D wave features are also observed as the surface waves pass through the barriers.

INTRODUCTION

The use of submerged structures like vertical barriers as breakwaters has been emphasized in different problems related to offshore structures for a long time. Because a submerged breakwater does not in general partition the natural sea, it is favored from the point of view of a marine scenario. Another significant reason for the submerged breakwater is that free exchange of water mass through the structures is necessary so that the water in the sheltered region can be kept circulating and therefore prevent stagnation and pollution (Yu and Chwang 1994). Moreover, in order to reduce the hydrodynamic pressure on both sides of the breakwaters, a porous breakwater is often an ideal choice.

Very often it is required to remove the unwanted waves from the high sea that are reflected by the seawall, and in such circumstances reduction of wave forces on the shoreline is important. Some rigid breakwaters have collapsed due to high wave impact loading (Su 1993; Franco 1994). Breakwaters made of material having fine pores normally experience reduced hydrodynamic pressures, and they also reduce the reflection of waves that are incident on the breakwater.

Another factor associated with the study of porous breakwaters is related to experimental surface wave studies. A major problem associated with experiments in narrow tanks is the unwanted wave reflection. One way to avoid this is to use porous screens that will dissipate the wave energy.

Although the scattering of water waves by obstacles that extend from the free surface to the bottom has received much attention due to their applications in different branches of engineering, the scattering of water waves by vertical porous barriers with mixed boundary conditions has not received much attention in the literature. Macaskill (1979) converted the boundary-value problems associated with the scattering of water waves by permeable thin barriers to integrodifferential equations by a suitable application of Green's integral theorem. However, no solution was obtained when the porosity of the barrier was taken into account. Chwang (1983) developed a porous wavemaker theory to study the problem of the generation of water waves by the harmonic oscillation of a thin permeable plate immersed in water of finite depth. Since then, many researchers [see Chwang and Chan (1998) and references therein] have used Chwang's theory to study more general problems of a similar type and obtained closed-form solutions.

Yu and Chwang (1994) investigated numerically the problem of reflection and transmission of water waves by a horizontally submerged plate in water of finite depth. Recently, Sahoo (1998) investigated the scattering of water waves by barriers of small porosity in water of infinite depth using the perturbation analysis. Porter and Evans (1995) studied the scattering of oblique incident water waves on a partially submerged barrier by the Galerkin method and obtained the reflection and transmission coefficients approximately in the case of finite water depth. They showed that the finite angle of incidence reduced the wave reflection, and it increased the transmission of waves because of the obstacles. However, the discrepancy of this method is that no full solution can be obtained by any suitable application of this method.

Losada et al. (1992) investigated the scattering of oblique incident water waves by rigid barriers in water of finite depth for various configurations of the barrier using the eigenfunction expansion method and the method of least-squares approximation. They obtained the reflection and transmission coefficients, but did not obtain any full solution. Nevertheless, this method certainly has the advantage that the velocity potential can be obtained completely. In the present study, the method of Losada et al. (1992) is used to study the scattering of oblique incident water waves by thin vertical permeable barriers in four different cases in finite water depth (Fig. 1):

- Type 1—a bottom-standing barrier
- Type 2—a surface-piercing barrier
- Type 3—a barrier with a gap
- Type 4—a submerged barrier

By application of the eigenfunction expansion method, the problems are converted into dual/triple series relations, and then the method of least-square approximation is applied to obtain the velocity potentials along with the reflection and transmission coefficients. Other characteristics such as the hydrodynamic pressure along the barrier and the surface wave amplitude are also investigated.

MATHEMATICAL FORMULATION

The problems under consideration are 3D in nature. Under the assumption of the linearized theory of surface waves, the problems are studied in the 3D Cartesian coordinate system. The fluid occupies the region $0 \leq y \leq h$, $-\infty < x, z < \infty$,

[1]Postdoctoral Fellow, Dept. of Mech. Engrg., Univ. of Hong Kong, Pokfulam Rd., Hong Kong.
[2]Asst. Prof., Dept. of Mech. Engrg., Univ. of Hong Kong, Pokfulam Rd., Hong Kong.
[3]Sir Robert H. Tung Chair, Dept. of Mech. Engrg., Univ. of Hong Kong, Pokfulam Rd., Hong Kong.

Note. Discussion open until January 1, 2001. To extend the closing date one month, a written request must be filed with the ASCE Manager of Journals. The manuscript for this paper was submitted for review and possible publication on November 10, 1998. This paper is part of the ***Journal of Waterway, Port, Coastal, and Ocean Engineering***, Vol. 126, No. 4, July/August, 2000. ©ASCE, ISSN 0733-950X/00/0004-0196–0205/$8.00 + $.50 per page. Paper No. 19635.

J. Waterway, Port, Coastal, Ocean Eng., 2000, 126(4): 196-205

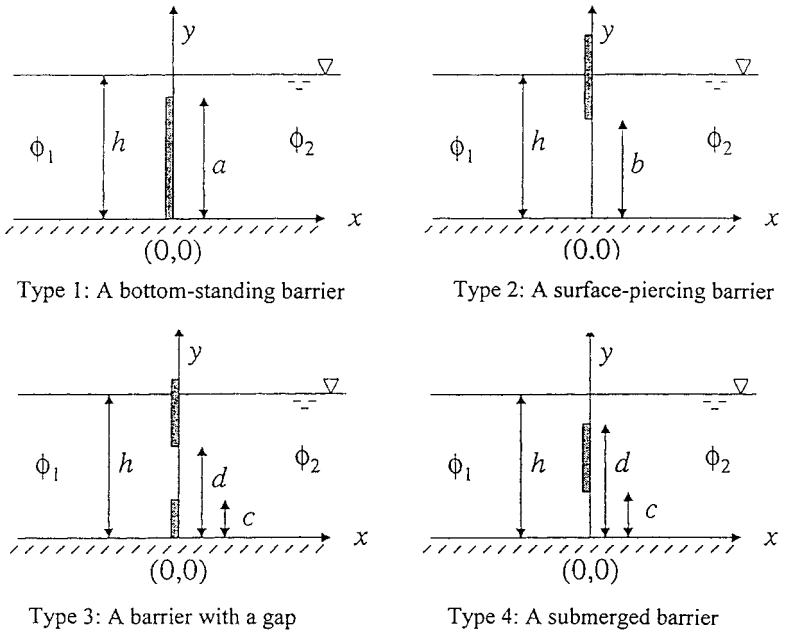

FIG. 1. Definition Sketch of Four Types of Permeable Barriers

except for the barriers in the fluid region. The barriers occupy the following positions (Fig. 1):

- Type 1: $x = 0$, $0 \le y \le a$
- Type 2: $x = 0$, $b \le y \le h$
- Type 3: $x = 0$, $0 \le y \le c$, $d \le y \le h$ with $c < d$
- Type 4: $x = 0$, $c \le y \le d$

We shall use the notation ''Bar'' for the barrier and ''Gap'' for the unobstructed gap along the line $x = 0$.

A progressive wave $\phi_I = \Re\{\phi_0 e^{i(k_0 x \cos\theta + k_0 z \sin\theta - \omega t)} \cosh k_{0y}\}$, with ϕ_0 being the velocity potential amplitude and ω the angular frequency of the wave, is assumed to be incident on the barrier. The wave number k_0 ($k_0 = 2\pi/\lambda$) satisfies the dispersion relation $\omega^2 = gk_0 \tanh k_0 h$ with g being the gravitational acceleration and λ the wavelength. The incident wave angle θ is measured relative to the normal of the barrier. Because a part of the wave is reflected and another part is transmitted, this suggests the existence of a velocity potential $\Phi[x, y, z, t]$ of the form $\Phi[x, y, z, t] = \Re\{\phi[x, y] e^{i(k_0 z \sin\theta - \omega t)}\}$ with $\phi[x, y]$ satisfying the partial differential equation

$$\left(\frac{\partial^2}{\partial x^2} + \frac{\partial^2}{\partial y^2} - \nu^2\right)\phi = 0 \quad \text{(in the fluid region)} \tag{1}$$

along with the linearized free surface boundary condition

$$\frac{\partial \phi}{\partial y} - K\phi = 0 \quad \text{on} \quad y = h \tag{2}$$

with $\nu = k_0 \sin\theta$; and $K = \omega^2/g$.

The condition on the porous barrier is given by Chwang (1983), based on Darcy's assumption

$$\frac{\partial \phi}{\partial x} = ik_0 G(\phi_1 - \phi_2) \quad \text{on} \quad x = 0, \quad y \in \text{Bar} \tag{3}$$

where $G = b\rho\omega/\mu k_0$ = porous-effect parameter defined by Chwang (1983) or the so-called Chwang parameter; b = material constant having the dimension of length; ρ = constant density of the fluid; and μ = constant coefficient of dynamic viscosity. The subscripts 1 and 2 denote the left and right side of the barrier, respectively.

The continuity of velocity and pressure along the gap are given by

$$\phi, \frac{\partial \phi}{\partial x} \quad \text{continuous on} \quad x = 0, \quad y \in \text{Gap} \tag{4}$$

The radiation and bottom boundary conditions are of the form

$$\phi[x, y] = \phi_0 \cosh k_0 y\{e^{i\xi x} + A_0 e^{-i\xi x}\} \quad \text{as} \quad x \to -\infty \tag{5}$$

$$\phi[x, y] = B_0 \phi_0 \cosh k_0 y e^{i\xi x} \quad \text{as} \quad x \to \infty \tag{6}$$

$$\frac{\partial \phi}{\partial y} = 0 \quad \text{on} \quad y = 0 \tag{7}$$

where A_0 and B_0 = unknown reflection and transmission coefficients to be determined, respectively; and $\xi = k_0 \cos\theta$.

METHOD OF SOLUTIONS

The velocity potential $\phi[x, y]$ satisfying (1) along with the boundary conditions (2) and (5)–(7) can be written in the form

$$\phi_1[x, y] = \phi_0 \cosh k_0 y\{e^{i\xi x} + A_0 e^{-i\xi x}\} + \sum_{n=1}^{\infty} \phi_0 A_n e^{p_n x} \cos k_n y, \quad x < 0 \tag{8}$$

$$\phi_2[x, y] = \phi_0 B_0 \cosh k_0 y e^{i\xi x} + \sum_{n=1}^{\infty} \phi_0 B_n e^{-p_n x} \cos k_n y, \quad x \ge 0 \tag{9}$$

where $p_n = \sqrt{k_n^2 + \nu^2}$; and A_n and B_n ($n = 1, 2, \ldots$) = coefficients corresponding to the evanescent wave modes in Regions 1 and 2, respectively. The wave numbers k_n satisfy the dispersion relations for evanescent wave modes

$$\omega^2 + gk_n \tan k_n h = 0 \quad \text{for} \quad n = 1, 2, \ldots \tag{10}$$

Using the condition that the velocity (i.e., $\partial\phi/\partial x$) is continuous along the barrier as well as along the gap, we derive that

$$A_0 + B_0 = 1, \quad A_n + B_n = 0 \quad \text{for} \quad n = 1, 2, \ldots \tag{11}$$

Again, substituting (8) and (9) in (3) along the barrier and then in (4) along the gap, we obtain that

J. Waterway, Port, Coastal, Ocean Eng., 2000, 126(4): 196-205

$$\sum_{n=0}^{\infty} A_n f_n[y] - f[y] = 0 \quad \text{for} \quad 0 \le y \le h \tag{12}$$

where

$$f_0[y] = i(\xi + 2k_0G)\cosh k_0 y, \quad y \in \text{Bar}$$

$$f_0[y] = \cosh k_0 y, \quad y \in \text{Gap}$$

$$f_n[y] = -(p_n - 2ik_0G)\cos k_n y \quad \text{for} \quad n = 1, 2, \ldots, \quad y \in \text{Bar}$$

$$f_n[y] = \cos k_n y \quad \text{for} \quad y \in \text{Gap}$$

$$f[y] = \cancel{2ik_0G}\cosh k_0 y, \quad y \in \text{Bar}$$

$$f[y] = 0 \quad \text{for} \quad y \in \text{Gap}$$

Writing

$$F[y] = \sum_{n=0}^{N} A_n f_n[y] - f[y] \tag{13}$$

we have by application of the least-squares method

$$\int_0^h |F[y]|^2 \, dy = \text{minimum} \tag{14}$$

Minimizing the above integral with respect to each A_m leads to the following:

$$\int_0^h F_m[y] F^*[y] \, dy = 0, \quad m = 0, 1, 2, \ldots, N \tag{15}$$

where

$$F_m[y] = \frac{\partial F(y)}{\partial R_m} = f_m[y], \quad F^*[y] = \sum_{n=0}^{N} A_n^* f_n^*[y] - f^*[y]$$

with $*$ denoting the complex conjugate.

Substituting for $F^*[y]$ and $F_m[y]$ in (15), we derive that

$$\sum_{n=0}^{N} X_{mn} A_n^* = b_m \quad \text{for} \quad m = 0, 1, 2, \ldots, N \tag{16}$$

which is a system of linear equations for the determination of A_n^*, with X_{mn} and b_m given by

$$X_{mn} = \int_0^h f_n^*[y] f_m[y] \, dy; \quad b_m = \int_0^h f^*[y] f_m[y] \, dy \tag{17a,b}$$

NUMERICAL RESULTS AND DISCUSSION

From (16) a complex $(N + 1) \times (N + 1)$ system of equations is obtained that can be solved. Although the number of terms required to guarantee a given accuracy varies with geometry and configurations (Wu 1973), in a preliminary trial test for convergence, it is found that even 5–10 terms are sufficient to ensure convergence to five-decimal places for the reflection coefficient $|A_0|$ for most cases under study. Only when the barrier is of smaller but finite normalized length, then a larger matrix size (25–30) is required for convergence to the same order of accuracy. In this study, we have chosen $N = 49$ for the matrix in all cases for uniformity. We list in Table 1 the modulus of the reflection coefficient $|A_0|$ for three of the many cases we tested with C as defined in (18).

In many previous works, the properties of orthogonality are invoked to construct a system of equations to find the coefficients. However, it is known that it is not possible to construct an orthogonal set for complicated configurations like multiple slits or gaps within a full barrier. Even when the orthogonal set is found, it is well known that convergence of the series is fairly slow. The beauty of this eigenfunction expansions and least-squares method is that it can be applied to many problems of a similar nature of the aforementioned configurations and is done so efficiently.

Bottom-Standing Barrier

We investigate first the effect of barrier length on the reflection coefficient. Fig. 2 shows that the reflection coefficient

TABLE 1. Values of $|A_0|$ for Various Values of N with $G = 0.5$, $C = 1$, $\theta = 45°$

	$\lvert A_0 \rvert$		
$N + 1$ (1)	Type 1 ($a = 1$) (2)	Type 1 ($a = 0.5$) (3)	Type 2 ($b = 0.5$) (4)
5	0.29788	0.08950	0.13375
10	0.29788	0.08634	0.12369
15	0.29788	0.08551	0.11911
20	0.29788	0.08523	0.11786
25	0.29788	0.08488	0.11688
30	0.29788	0.08484	0.11685
35	0.29788	0.08483	0.11685
40	0.29788	0.08483	0.11684
45	0.29788	0.08483	0.11684

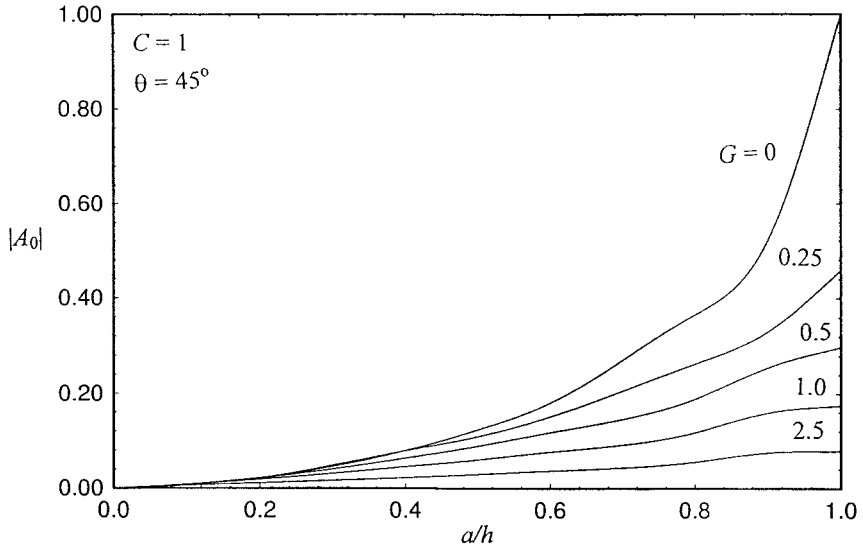

FIG. 2. Variation of Reflection Coefficient $|A_0|$ versus Dimensionless Barrier Length a/h for Various Values of Porous-Effect Parameter G for Type 1 Barrier, $C = 1$, $\theta = 45°$

J. Waterway, Port, Coastal, Ocean Eng., 2000, 126(4): 196-205

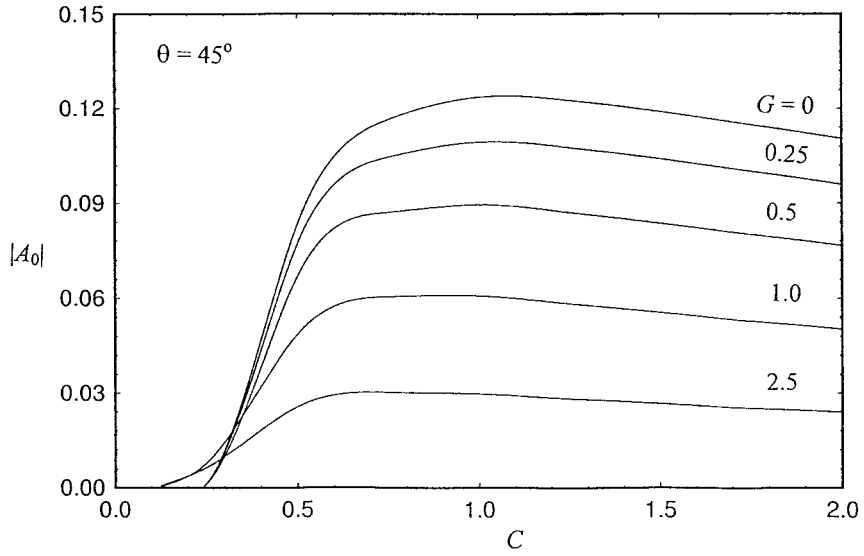

FIG. 3. Variation of Reflection Coefficient $|A_0|$ versus Wave-Effect Parameter *C* for Various Values of Porous-Effect Parameter *G* for Type 1 Barrier, $a/h = 0.5$, $\theta = 45°$

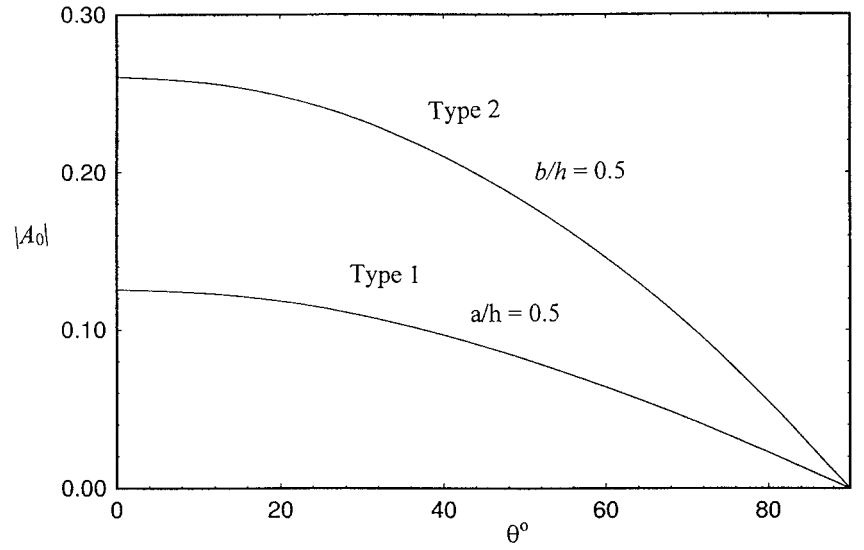

FIG. 4. Variation of Reflection Coefficient $|A_0|$ versus Incident Wave Angle θ for Type 1 and Type 2 Barriers, $G = 0.5$, $C = 1$

increases with the dimensionless barrier length a/h. This is within physical understanding, as a longer barrier will certainly reduce transmission of wave energy. However, in all the cases considered, it seems that the rise of the reflection coefficient with respect to a/h is not significantly large until a/h is about 0.75. It is because the wave energy is mostly concentrated on the free surface, and so a short barrier will have little effect in restricting the wave energy transmission. Also, it can be seen that the reflection coefficient decreases with increasing G for fixed a/h. This agrees again with the physical intuition, because larger permeability (larger G) allows more fluid and energy to pass through the barrier. In the limit, when $G = 0$ corresponding to an impermeable barrier and $a/h = 1$, all energy is being reflected, and thus $|A_0| = 1$, simply meaning a total partitioning of the sea.

Fig. 3 shows the variation of the reflection coefficient versus the wave-effect parameter C for various porous-effect parameters G and a fixed barrier length $a/h = 0.5$. The wave-effect parameter C is defined by Chwang (1981) as

$$C = \frac{g}{\omega^2 h} \tag{18}$$

which is a comparison between gravitational effect and oscillation effect. The reflection coefficient behaves as a convex function with respect to C. Almost total transmission occurs when the wave-effect parameter C is small, and this agrees with the numerical results of Losada et al. (1992), which were shown to agree with the experimental data of Ogilvie (1960). This can be attributed to the fact that the wave-effect parameter is a comparison of the gravitational force to the unsteady force of the incident waves. When C is small, transmission is enhanced by the slowness of oscillation due to the uniform behavior of potential far from the barrier (Tuck 1975). When C is large, gravitational force is dominant, and thus the transmission of wave energy is also retarded. The combined effect of the unsteady force and gravitational force results in the variation of the reflection coefficient.

Fig. 4 shows the variation of the reflection coefficient versus incident wave angle θ. The continual decrease of reflection coefficient with respect to the incident angle is anticipated. This has been found in previous works involving impermeable (Losada et al. 1992) or porous breakwaters (Dalrymple et al. 1991). However, we did not locate a kink minimum for the reflection coefficient as in the results of Dalrymple et al.

J. Waterway, Port, Coastal, Ocean Eng., 2000, 126(4): 196-205

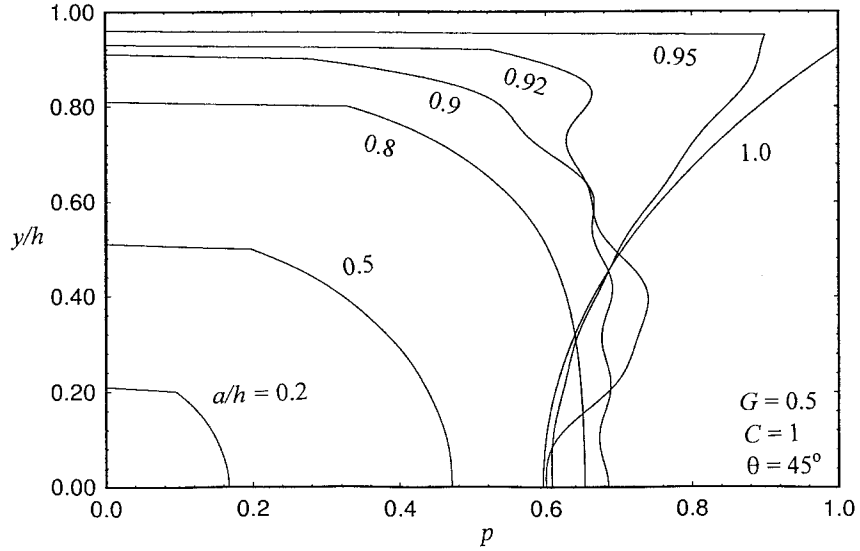

FIG. 5. Normalized Pressure Force *p* versus Vertical Height *y*/*h* for Various Values of Barrier Length *a*/*h*, *G* = 0.5, *C* = 1, θ = 45°

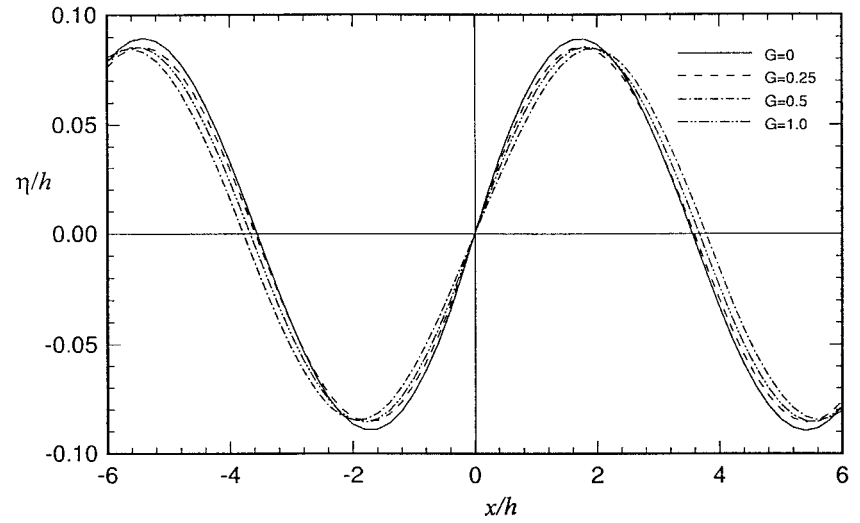

FIG. 6. Normalized Wave Amplitude η/*h* for Various Values of Porous-Effect Parameter *G* for Type 1 Barrier, *C* = 1, θ = 45°, *a*/*h* = 0.5

(1991). We believe this is due to the fact that our analysis does not include an inertial factor as in Sollitt and Cross (1972) and in Dalrymple et al. (1991).

Fig. 5 shows the variation of the hydrodynamic pressure force acting on the permeable barrier versus vertical distance *y*/*h* for various barrier lengths *a*/*h*. The normalized pressure force *p* is defined by $(\phi_1[0, y] - \phi_2[0, y])/\sqrt{C}\phi_0$. For a smaller barrier, the pressure force decreases monotonically with vertical distance. Also discovered is that the larger the length of the barrier, the larger the magnitude of the force as the barrier is reacting to more wave energy impact. A finite value of force is also assumed at the tip of the barrier, due to the flow. However, when the barrier length *a*/*h* approaches 1, the variation starts to change drastically. The pressure force exhibits some form of ''instability'' (*a*/*h* = 0.9) and changes at some point from a monotonically decreasing function to a monotonically increasing one with respect to vertical height *y*/*h*. This is due to the cosh $k_0 y$ term that becomes increasingly dominant when compared with the evanescent wave modes for larger *y*/*h*. The variation of sign of the pressure gradient is a resultant of wave energy distribution due to partial transmission and partial reflection by the porous barrier. The sign obviously depends on the amount of energy partitioned by the barrier.

Fig. 6 shows the wave amplitude along the *z* = 0 plane for *a*/*h* = 0.5 and θ = 45°. Because the barrier is submerged in the sea in addition to its relatively short length, its effect is not very significant. However, a contour plot shows that, although the barrier is assumed to be infinitely long in the *z*-direction, 3D features on the surface waves occur as the waves pass the barrier. 3D local maxima and minima are observed in Fig. 7 as the waves pass the barrier from left to right. This is due perhaps to the combination of the retardation of the surface waves at the bottom due to the barrier and the incident waves passing above the barrier. The two superimposed together with a certain phase-shift, thus resulting in this 3D waveform.

Surface-Piercing Barrier

A Type 2 barrier or a surface-piercing barrier is the complementary case of Type 1, and thus by intuition, we expect most of the results of a Type 2 barrier would be complementary to that of a Type 1. In Fig. 8, all of the reflection coefficients decrease monotonically with respect to increasing gap length *b*/*h*. More interesting to note is that for large values of *G*, the decrease is actually very slow, illustrating that the dif-

J. Waterway, Port, Coastal, Ocean Eng., 2000, 126(4): 196-205

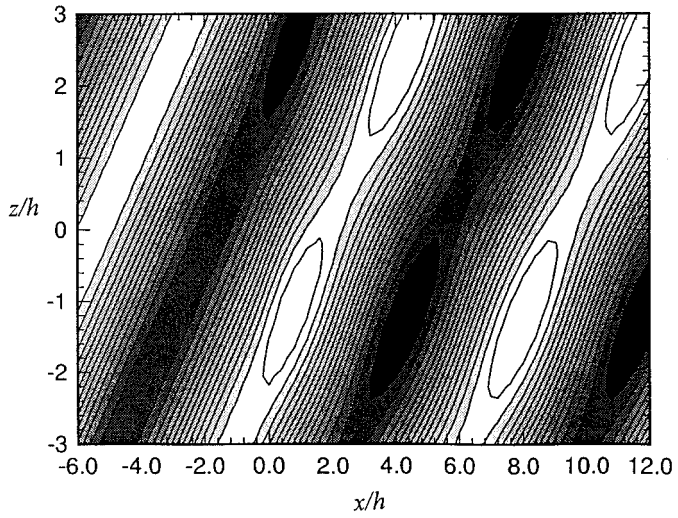

FIG. 7. Contour Plot of Surface Waves past Type 1 Barrier, *a*/*h* = 0.5, *G* = 0.5, *C* = 1, θ = 45°

ference in blockage of energy between a long barrier and a short barrier is actually quite small, if the barrier extends from the free surface to the bottom. This is attributable to the surface wave energy being concentrated mostly near the free surface, and thus the bottom portion of the barrier does little to reflect wave energy.

Fig. 9 shows the variation of the reflection coefficient versus the wave-effect parameter for gap length $b/h = 0.5$. It can be seen that the reflection coefficient drops monotonically with respect to the wave-effect parameter, with its value also decreasing with increasing G. From this, it can be deduced that a Type 2 barrier is more efficient in blocking the penetration of short-wavelength surface waves.

Fig. 10 shows the surface wave profile for surface waves passing through a Type 2 barrier. It is observed that at the barrier a discontinuity exists between the incident wave and the transmitted wave. This discontinuity decreases with increasing G, which agrees with physical intuition. This discontinuity was also noticed by Lee and Chwang's (1997) and Ursell (1947). However, being a thin permeable barrier, it might be difficult to envisage a discontinuity of wave transmission. We believe such a dilemma is attributed to the idealization of

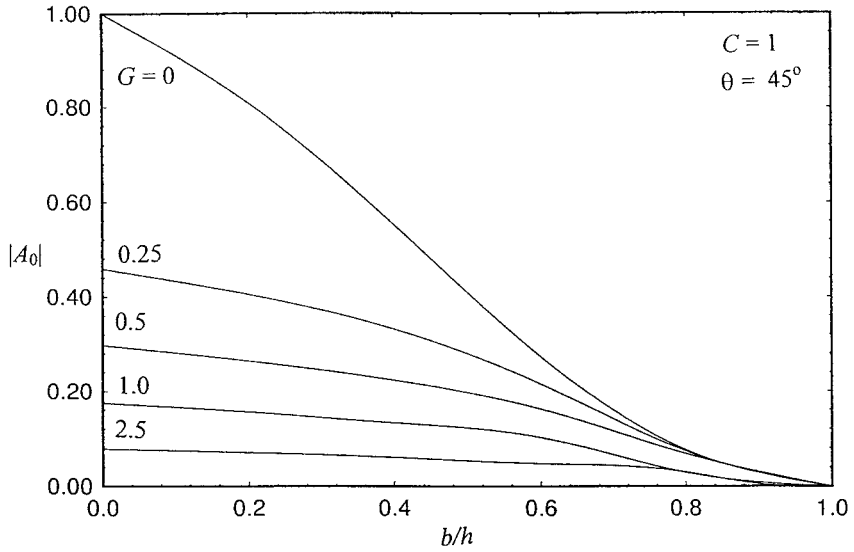

FIG. 8. Variation of Reflection Coefficient $|A_0|$ versus Gap Length *b*/*h* for Various Values of *G* for Type 2 Barrier, *C* = 1, θ = 45°

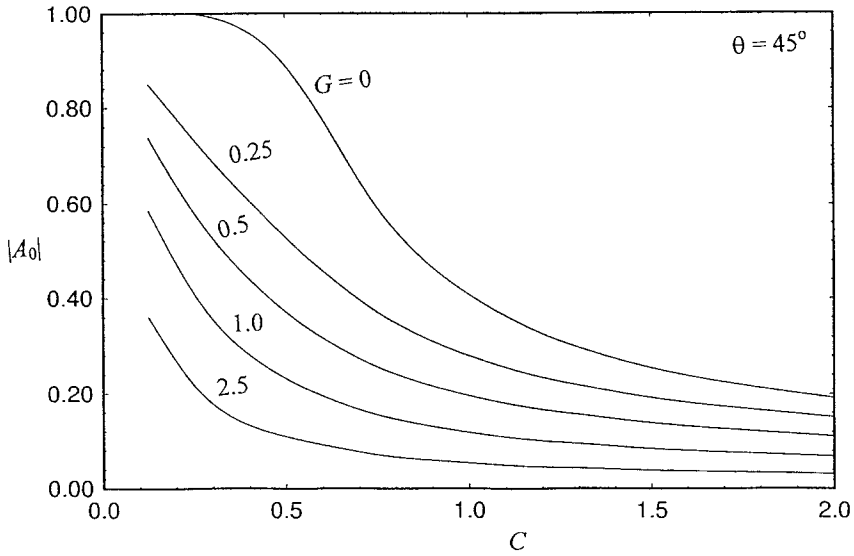

FIG. 9. Variation of Reflection Coefficient $|A_0|$ versus Wave-Effect Parameter *C* for Various Values of *G* for Type 2 Barrier, *b*/*h* = 0.5, θ = 45°

J. Waterway, Port, Coastal, Ocean Eng., 2000, 126(4): 196-205

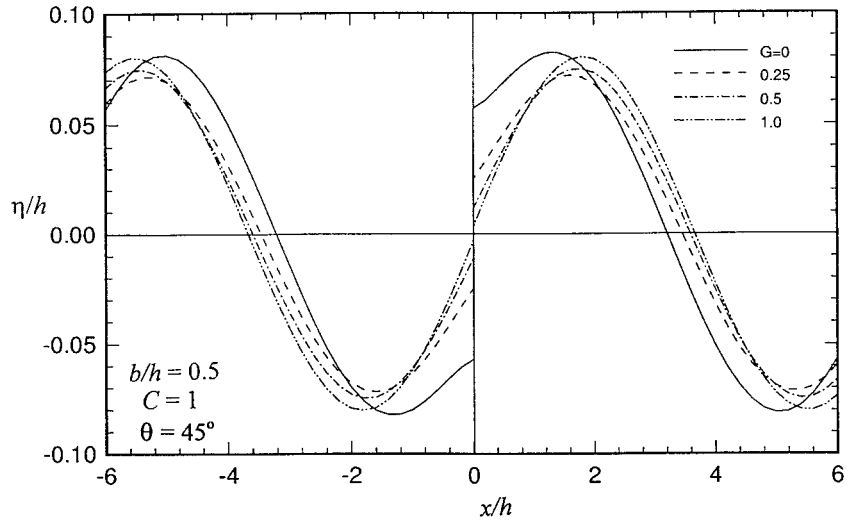

FIG. 10. Normalized Surface Wave Changes for Various Values of *G* for Type 2 Barrier, $C = 1$, $\theta = 45°$

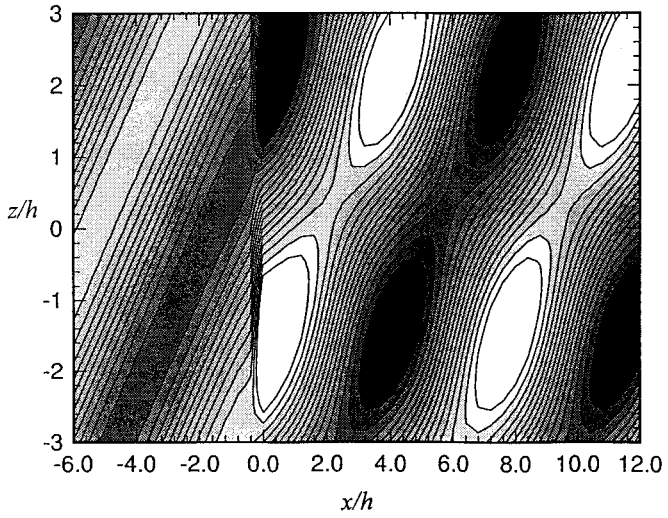

FIG. 11. Contour Plot of Surface Waves past Type 2 Barrier, $b/h = 0.5$, $G = 0.5$, $C = 1$, $\theta = 45°$

an infinitely thin barrier, and to resolve it we might need to extend our studies to surface waves within the porous block. 3D wave features are again observed as the waves pass through the barrier as in Fig. 11.

Barrier with Gap

We now consider the third type of barrier, in which a gap of width $(d - c)$ exists midway between the barrier that extends from the free surface to the sea bottom. The configuration is similar to Tuck's consideration (1975), except that the barrier we consider is now permeable.

Fig. 12 shows the variation of the reflection coefficient versus gap length $(d - c)/h$ for various values of the porous-effect parameter G. Increasing gap length $(d - c)/h$ means reducing reflection, and thus reflection coefficients are seen to decrease monotonically with gap length. As predicted, the trend is fairly similar to a Type 2 barrier, because the barrier under the gap can do very little to reflect surface waves.

The variation of the reflection coefficient versus the wave-effect parameter C also shows similar characteristics to a Type 2 barrier. Moreover, reflection is preferentially higher for

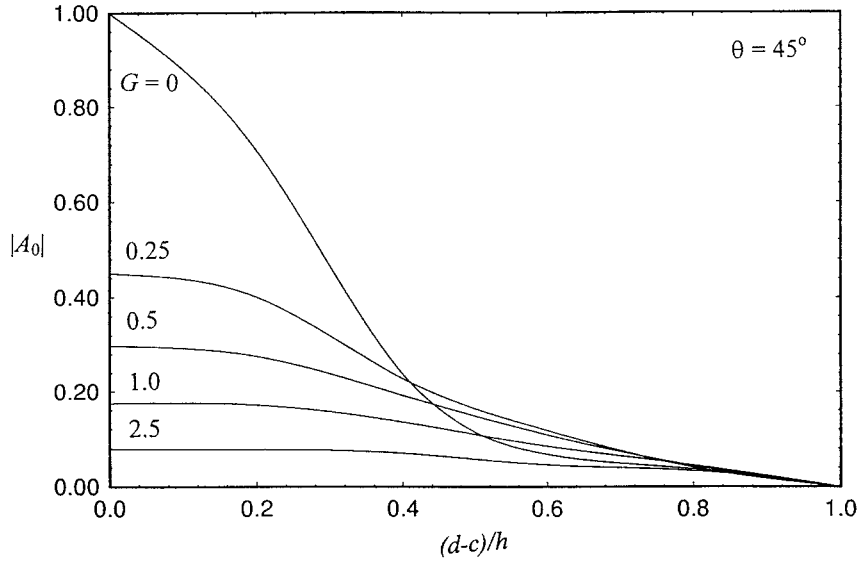

FIG. 12. Variation of Reflection Coefficient $|A_0|$ versus Gap Length $(d - c)/h$ for Various Values of *G* for Type 3 Barrier, $C = 1$, $\theta = 45°$

J. Waterway, Port, Coastal, Ocean Eng., 2000, 126(4): 196-205

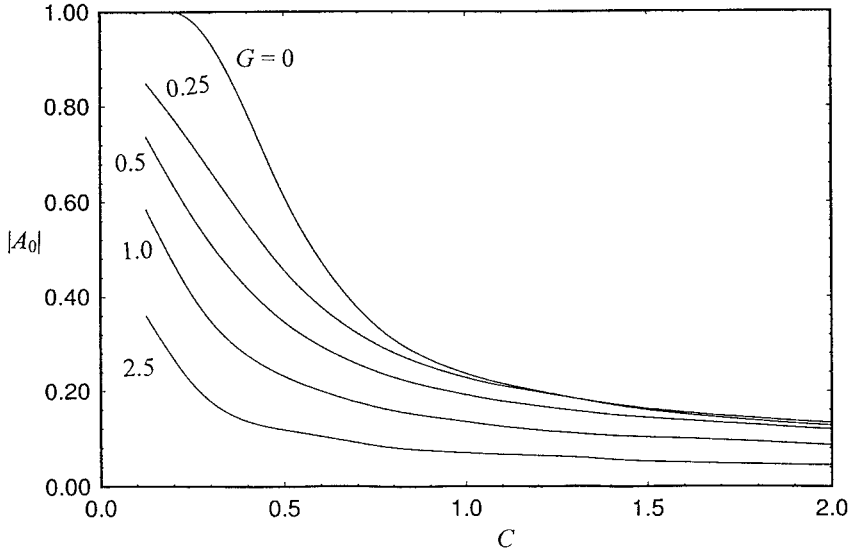

FIG. 13. Variation of Reflection Coefficient $|A_0|$ versus Wave-Effect Parameter C for Various Values of G for Type 3 Barrier, $(d - c)/h = 0.6$, $\theta = 45°$

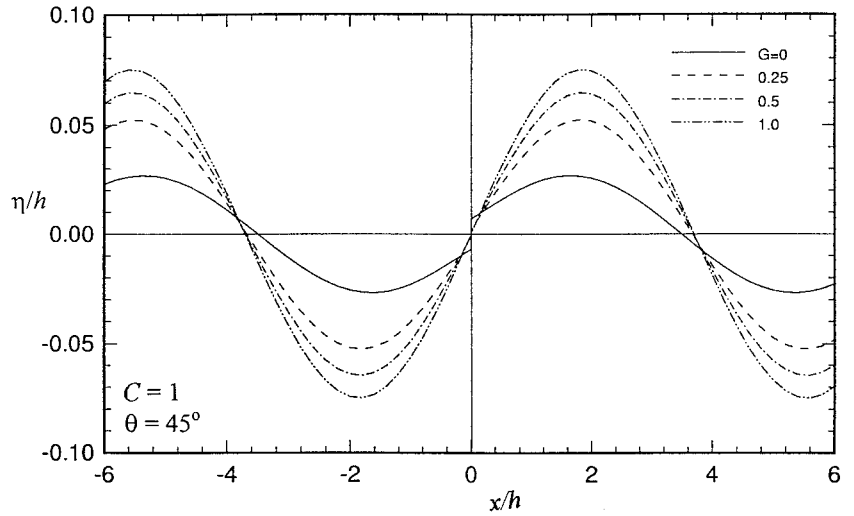

FIG. 14. Normalized Surface Wave Changes for Various Values of G for Type 3 Barrier, $(d - c)/h = 0.6$, $C = 1$, $\theta = 45°$

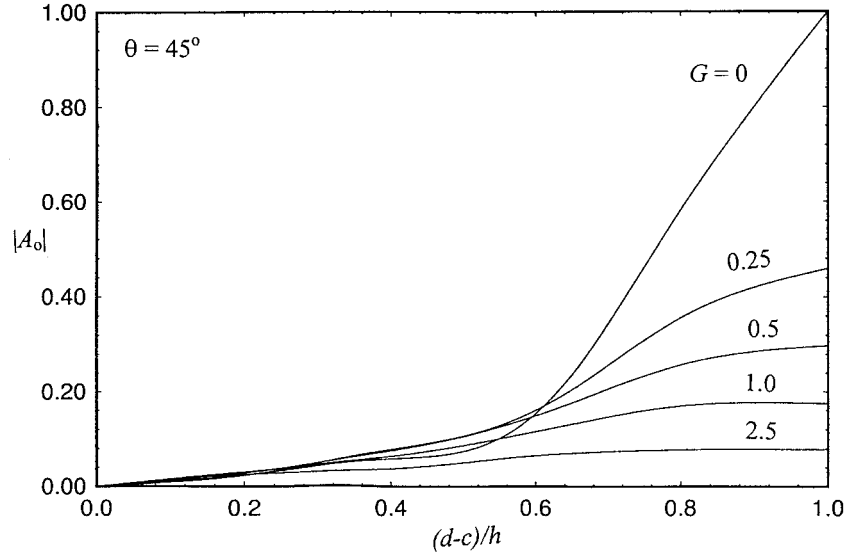

FIG. 15. Variation of Reflection Coefficient $|A_0|$ versus Normalized Barrier Length $(d - c)/h$ for Various Values of G for Type 4 Barrier, $C = 1$, $\theta = 45°$

J. Waterway, Port, Coastal, Ocean Eng., 2000, 126(4): 196-205

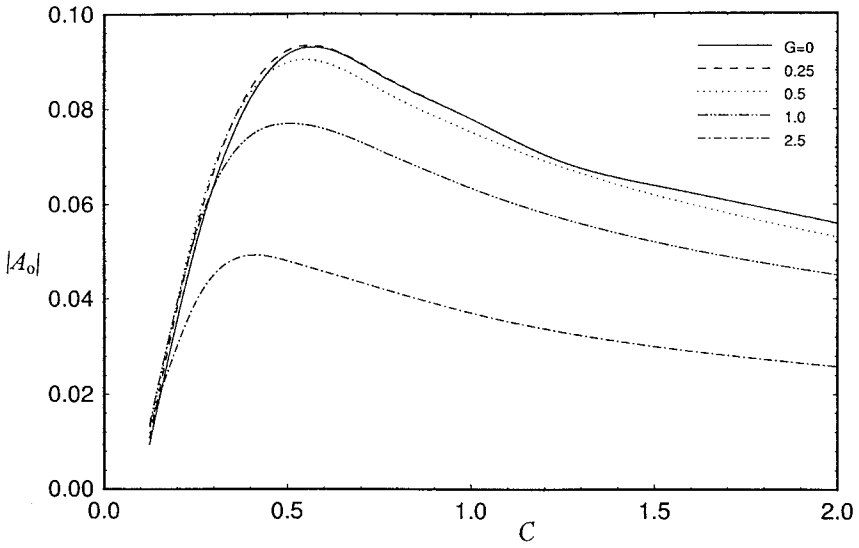

FIG. 16. Variation of Reflection Coefficient $|A_0|$ versus Wave-Effect Parameter *C* for Various Values of *G* for Type 4 Barrier, $(d - c)/h = 0.6$, $\theta = 45°$

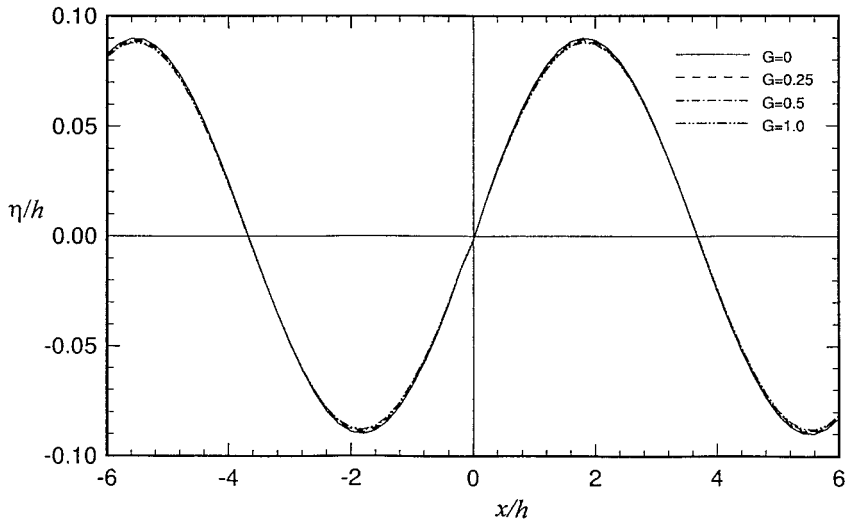

FIG. 17. Normalized Surface Wave Changes for Various Values of *G* for Type 4 Barrier, $(d - c)/h = 0.6$, $C = 1$, $\theta = 45°$

shorter-wavelength waves, as it is difficult for the barrier to ''feel'' the longer waves, as shown in Fig. 13.

The free surface elevation is plotted in Fig. 14 for $(d - c)/h = 0.6$. All wave trains are continuous for a finite value of G. Only in the case of zero G does a discontinuity exist along the surface waves. This result is unexpected, as we anticipated that some discontinuity would be observed when the barrier is at the free surface for finite values of G, just as a Type 2 barrier. We attribute this result to the fact that the gap is large enough [$(d - c)/h = 0.6$] for most energy to pass through easily.

Submerged Barrier

We now consider the fourth type of barrier, in which a barrier of width $(d - c)$ is located midway between the free surface and the sea bottom. The variations of the reflection coefficients versus the barrier length $(d - c)/h$ and the wave-effect parameter C are shown in Figs. 15 and 16, respectively. As anticipated, they show similar trends to a Type 1 barrier due to configuration similarity. The surface waves seem unaffected by the immersed barrier for various values of the porous-effect parameter G for a barrier length of 0.6 as shown in Fig. 17. We believe that this is due to the ineffectiveness of the barrier when submerged at a distance and its short length.

CONCLUSIONS

The scattering of obliquely incident surface waves by permeable vertical barriers in water of finite depth is investigated for four different configurations of the barriers. The multiple series relations of the eigenfunction expansion method and the least-square approximation are effective tools in analyzing problems of this type. This method is also applicable to the analysis of similar problems with more complicated configurations.

The reflection coefficients, hydrodynamic pressure differences along the two sides of the barriers, and surface elevations are obtained for different values of the wave-effect parameter, the porous-effect parameter, and the angle of incidence. It is observed that the finite angle of incidence and the porous effect of the barriers reduce the reflection of incident waves, the wave amplitude, and the hydrodynamic pressure exerted on the barriers. 3D features of surface waves are observed as surface waves pass through the porous barriers.

The present work represents a first step in the study of porous breakwaters. Porous breakwaters of finite width or of a different geometric cross section are suggested for further re-

J. Waterway, Port, Coastal, Ocean Eng., 2000, 126(4): 196-205

search. However, the geometries of these configurations pose great mathematical challenges, and this work will be investigated in the near future.

ACKNOWLEDGMENT

This research work was sponsored by the Hong Kong Research Grants Council under Grant Nos. HKU 304/95E and HKU 568/96E.

APPENDIX. REFERENCES

Chwang, A. T. (1981). ''Effect of stratification on hydrodynamic pressures on dams.'' *J. Engrg. Mathematics*, 15, 49–73.

Chwang, A. T. (1983). ''A porous wavemaker theory.'' *J. Fluid Mech.*, Cambridge, U.K., 132, 395–406.

Chwang, A. T., and Chan, A. T. (1998). ''Interaction between porous media and wave motion.'' *Annu. Rev. of Fluid Mech.*, 30, 53–84.

Dalrymple, R. A., Losada, M. A., and Martin, P. A. (1991). ''Reflection and transmission from porous structures under oblique wave attack.'' *J. Fluid Mech.*, Cambridge, U.K., 224, 625–644.

Franco, L. (1994). ''Vertical breakwaters: The Italian experience.'' *Coast. Engrg.*, 22, 31–55.

Lee, M. M., and Chwang, A. T. (1997). ''Transmission and reflection of water waves by a partially submerged porous barrier.'' *Proc., 7th Asian Congr. of Fluid Mech.*, Applied Publishers, New Delhi, India, 573–576.

Losada, I. J., Losada, M. A., and Roldán, A. J. (1992). ''Propagation of oblique incident waves past rigid vertical thin barriers.'' *Appl. Oc. Res.*, 14, 191–199.

Macaskill, C. (1979). ''Reflection of water waves by permeable barrier.'' *J. Fluid Mech.*, Cambridge, U.K., 95, 141–157.

Ogilvie, T. F. (1960). ''Propagation of waves over an obstacle in water of finite depth.'' Institute of Engineering Research Series No. 82, University of California, Berkeley, Calif.

Porter, R., and Evans, D. V. (1995). ''Complementary approximations to wave scattering by vertical barriers.'' *J. Fluid Mech.*, Cambridge, U.K., 294, 155–180.

Sahoo, T. (1998). ''On the scattering of water waves by porous barriers.'' *Zeitschrift für Angewandte Mathematik and Mechanik*, Berlin, Germany, 78(5), 364–370.

Sollitt, C. K., and Cross, R. H. (1972). ''Wave transmission through permeable breakwaters.'' *Proc., 13th ASCE Conf. of Coast. Engrg.*, Vol. 3, ASCE, New York, 1827–1846.

Su, C. H. (1993). ''Wave dissipation of porous wave absorber with application to harbour oscillation.'' PhD thesis, National Cheng Kung University, Taiwan.

Tuck, E. O. (1975). ''Matching problems involving flow through small holes.'' *Adv. in Appl. Mech.*, C. S. Yih, ed., Academic, New York, 15, 89–157.

Ursell, F. (1947). ''The effect of a fixed vertical barrier on surface waves in deep water.'' *Proc., Cambridge Philosophical Soc.*, Cambridge, U.K., 43, 374–382.

Wu, C. P. (1973). ''Variation and iterative methods for waveguides and arrays.'' *Computational techniques for electromagnetics*, Pergamon, London, 266–304.

Yu, X., and Chwang, A. T. (1994). ''Wave motion through porous structures.'' *J. Engrg. Mech.*, ASCE, 120(5), 989–1008.